

# We are IntechOpen, the world's leading publisher of Open Access books Built by scientists, for scientists

**5,000**

Open access books available

**125,000**

International authors and editors

**140M**

Downloads

Our authors are among the

**154**

Countries delivered to

**TOP 1%**

most cited scientists

**12.2%**

Contributors from top 500 universities



**WEB OF SCIENCE™**

Selection of our books indexed in the Book Citation Index  
in Web of Science™ Core Collection (BKCI)

Interested in publishing with us?  
Contact [book.department@intechopen.com](mailto:book.department@intechopen.com)

Numbers displayed above are based on latest data collected.

For more information visit [www.intechopen.com](http://www.intechopen.com)



# Thermal and Hydraulic Analysis of Transfer Medium Motion Regime in Flat Plate Solar Collector

*Yedilkhan Amirgaliyev, Murat Kunelbayev,  
Kalizhanova Aliya, Ainur Kozbakova,  
Omirlan Auelbekov and Nazbek Katayev*

## Abstract

In the research herein, we have considered the thermal and hydraulic analysis of transfer media motion mode in the flat solar collector. We have substantiated the thermal and hydraulic parameters of the flat plate solar collector. Heat absorbing flat solar collector tubes hydraulic analysis has shown, that using the heat transfer standard size there might be located the pipeline, the length of which 2.5 times more than of the collector's body, sufficiently increasing at that insolation time on the transfer media.

**Keywords:** flat plate solar collector, heat, hydraulics, transfer media

## 1. Introduction

Flat plate solar collector is a type of the heat exchanger, in which the liquid absorbs the energy from the solid surface, exposed to the solar radiation. Dependent on the potentially reached temperature, those equipment types might be classified according to the following parameters: low temperature, average temperature and high temperature. In the work herein we concentrate at low temperature solar collectors, where the maximum temperature, reached by the working liquid, lower, than 100°C. Those types devices thermal characteristic is based on defining the collector's performance and heat losses for the environment. Growing interest in cutting the capital cost of the systems thereof is focused at raising the thermal efficiency at the expense of optimizing the usage of materials for collectors' construction [1].

The work [2, 3] considers industrial applying the solar heating systems which needs considerable amount of hot water. In the research there has been investigated the usage of the solar collector sets, located sequentially, and the system has been experimentally tested to check its adequacy for providing the demanded thermal loading. The work [4] has studied the energy efficiency of independent and centralized heating systems accounting the solar plants integration; specified the energy specific consumption, additional power consumption, which reduces the

buildings energy performance. The work [4] has investigated the large-scale solar collector plant for using in hostels, pools, restaurants and production enterprises. The work has been focused at the assessing the performance, without accounting actual collectors' design and consumption capacity. The work [5] presents the integration of renewable power sources for a big meat company. There considered the renewable energy sources: solar power, biomass, some types of wastes and geothermal energy sources. Work [6] has studied the solar energy thermal integration in the process of fish canning applying the combined analysis and exergy analysis.

Pressure drop in water pipeline networks construction for energy distribution has been considered in [7], when there has been revealed, that the considerable energy saving might be reached using the pressure fall through the pressure management strategy in the network in the serial-parallel hydraulic circuit. The work [8] presents some solar water heating construction aspects, appropriate for big and regular demands to the hot water in hospitals and dormitories. There have been experimentally analyzed different schemes of the solar collectors switching ways, such as cascade, series, parallel and true parallel. Proceeding from the outcomes thereof the system with big number of solar collectors shows the maximum efficiency and economic feasibility. In the work [9] there has been conducted the economic assessment of industrial solar thermal plants in Greece. Also, we have considered the mathematical model of separate constructions and operation mode of thermosyphon circulation double circuit solar collector. Proceeding from the analysis results we have managed to optimize individual structural elements, as well, predicted the thermal regime and alternative solutions selection for designing the flat solar collectors and their operation regime selection [10]. In [11], the thermohydraulic performance parameter was calculated, which was used and presented to find a useful increase in thermal energy taking into account the equivalent thermal energy necessary for the production of working energy, as well as hydraulic losses as a result of expanded surfaces on the plate of the solar collector absorber were calculated. In [12], the influence of the shape of the absorber on the heat-hydraulic characteristics of the collector was studied for three general models with air flow. In [13], the experimental characteristics of the hydro-hydraulic parameters of compacted-bed solar air heaters were investigated. The parameter of thermohydraulic characteristics, called the "effective efficiency," was calculated, which was used to find a useful increase in thermal energy, taking into account the equivalent thermal energy. During the experimental work, it was observed that the thermo-hydraulic efficiency decreases with increasing values of the ratio of the layer depth to the size of the element and the porosity of the layer, but it increases with increasing mass air flow, reaches a maximum and subsequently decreases with a further increase in mass flow. In [14], optimization of thermohydraulic characteristics in tripartite artificially roughened solar air heaters was solved. The optimal thermo-hydraulic characteristics of such a solar air heater are both quantitatively and qualitatively better than that of single-sided rough solar air heaters. In [15], the thermohydraulic characteristics of a forced convection solar air heater using the surface of a fin absorber were investigated. The parameters of energy efficiency are experimentally calculated, such as absorbed thermal energy, thermal efficiency of a solar air heater, heat-hydraulic efficiency of an air heater. Verma and Prasad in [16] investigated the optimal thermo-hydraulic characteristics of solar air heaters, in which they determined the maximum heat transfer and the minimum pressure drop. Mittal and Varshney in [17] calculated the optimal thermo-hydraulic characteristics of a metal-mesh solar heater. In [18], an experimental study calculated the parameters of the thermal analysis of triangular glass covers with artificial triangular solar heaters.

The goal of the work hereby is to link the thermal project with hydraulic design to specify the location of the solar collectors which will correspond to both demanded thermal load and prescribed pressure drop.

## 2. Model of research

In the working hereby the researchers study the thermal and hydraulic analyses of transfer medium motion regime in the flat-plate solar collector.

To carry out the works the researchers analyzed a new flat solar collector, as well, experimentally investigated and substantiated the thermal and hydraulic transfer medium motion regime hydraulic parameters in the flat plate solar collector.

**Figure 1** shows the flat plate solar collector's model. Concept and novelty is in the fact, that in distinction from the known design principle, the collector contains a transparent glazed unit 2 with double glass and with a reduced pressure, as well, a parametric frame 1. Wooden frame bottom 7 is made of 8 mm thickness plywood with an attached heat sealing film 5 with foil. In the gap between the glazed unit and frame bottom there is lied a flexible thin-walled stainless corrugated tube in the coil form tubes edges are attached to output and input protruding tubes 6.

**Figure 1** demonstrates the flat plate solar collector mockup. Solar collector is the basic heat generating module of the solar plant. To achieve the set goal we have elaborated a principally new flat plate solar collector, based on which there will be constructed the standard series solar plants for water and buildings heating (**Figures 2–4** and **Table 1**).

Thermal mode in the solar collector elements is defined with the form and dimensions of its profile, thermal-physical properties of constituents parts and climatic conditions.

Heat exchanger's heat loading might be computed proceeding from the energy balance as [19]:

$$Q = mc\Delta T \quad (1)$$

where  $Q$ —heat loading,  $m$ —water flow,  $\Delta T$ —water temperature raising, prescribed ( $T_{\text{out}}-T_{\text{in}}$ ), where  $T_{\text{out}}$ —water output temperature, and  $T_{\text{in}}$ —inlet temperature. From the design equation and assuming, that the collector's absorbing surface is under the constant temperature ( $T$ ), the demanded surface square equals to [20]:

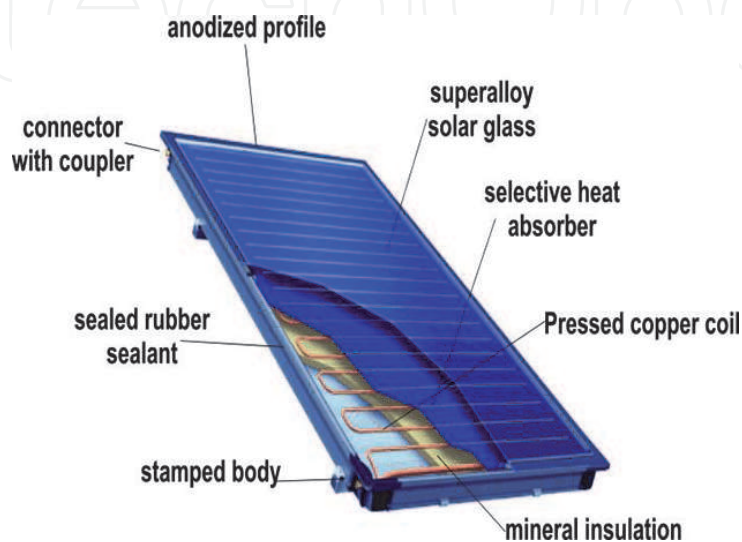


**Figure 1.**  
*Principal diagram of flat solar collector.*





**Figure 2.**  
Flat plate solar collector's mockup [12].

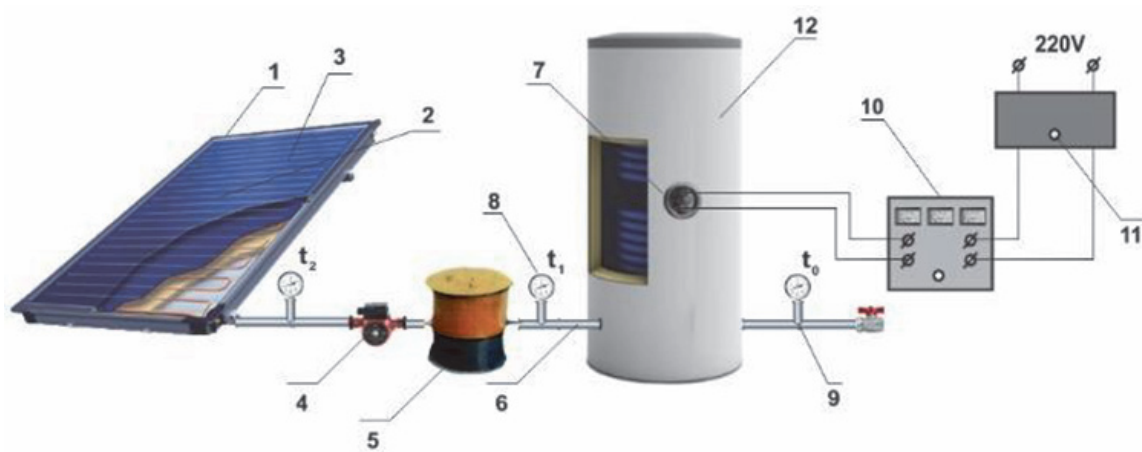


**Figure 3.**  
Principal diagram of solar heat supply: (1) thermally insulated body; (2) translucent covering; (3) tank-absorber; (4) circulating pump; (5) thermal pump; (6) pipeline; (7) tubular energy heating; (8, 9) thermometers for measuring the water temperature at inlet and outlet from a tank absorber and environment; (10) set of electric meters K 501; (11) autotransformer; (12) tank-accumulator; and (13) controller.

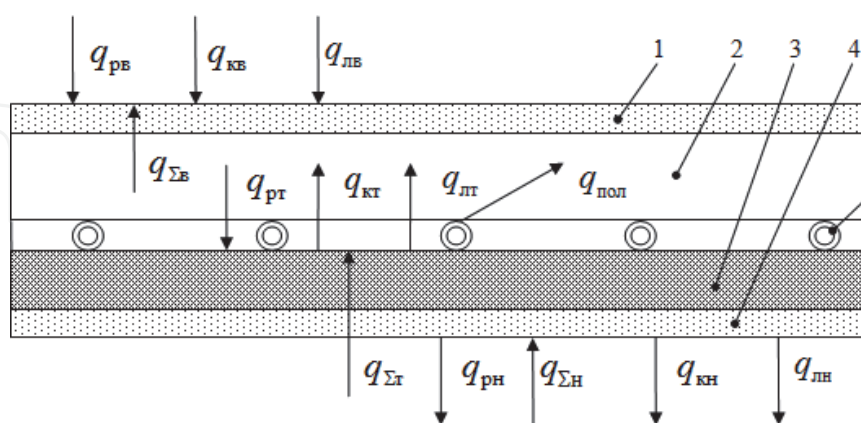


**Figure 4.**  
Diagram of thermal flows, passing via collector elements surfaces: (1) upper cover, made of translucent material; (2) gap spacing; (3) absorber; (4) lower cover (heat insulator); and (5) copper tubular spiral [12].

$$A = \frac{Q}{h\Delta T_{Lm}} \quad (2)$$

where  $A$ —heat transfer surface square,  $h$ —heat transfer film factor, and  $\Delta T_{Lm}$ —logarithmic mean temperature difference, accessible to the heat transfer. If the

Parameters	Value
Absorbing plate material	Copper
Absorber plate dimensions	2 m × 1 m
Plate thickness	0.4 mm
Glazing material	Hardened glass
Glazing dimensions	2 m × 1 m
Glazing thickness	4 mm
Insulation	Foam plex (foam, polyurethane)
Collector tilt angle	45°
Absorber's thermal conductivity	401 W/(m K)
Insulation thermal conductivity	0.04 W/(m K)
Transmittance-absorption factor	0.855
Sun apparent temperature	4350 K
Ambient temperature	303 K
Radiation intensity	1000 W/m <sup>2</sup>

**Table 1.**  
 Specifications of flat plate solar collector.

collector ( $A$ ) surface square is expressed as a member of the collector's geometry, then we obtain:

$$A = \pi d_i L_t N_t U_p \quad (3)$$

where  $d_i$ —tube inner diameter,  $N_t$ —tubes quantity per a collector, and  $U_p$ —collectors amount in parallel. Heat length ( $L_t$ ) is an exchanger length, necessary to satisfy the demanded loading. Uniting the Eqs. (1)–(3) and rearranging, we obtain the thermal length, which equals to

$$L_t = \frac{m C_p (T_{out} - T_{in})}{\pi d_i N_t U_p h \Delta T_{Lm}} \quad (4)$$

The film heat transfer factor might be computed according to a formula [21]:

$$h = \frac{4200(1.35 + 0.02)v^2}{d_i^{0.2}} \quad (5)$$

It is important to note, that in the above equation  $d_i$  shall be used in (mm);  $T$ —water temperature, and  $v$ —speed, which can be computed as follows:

$$v = \frac{m}{\rho A_c} \quad (6)$$

If the term  $\rho$ —water density, and  $A_c$ —free flow square, which might be expressed as:

$$A_c = \frac{\pi d_i^2}{4} N_t U_p \quad (7)$$

Hydraulic length ( $L_h$ ) is the heat exchanger length, necessary for conformity to the denoted pressure fall. Pressure fall at the heat exchanger core can be expressed as in [19]:

$$\Delta P = \frac{2f\rho L_h v^2}{d_i} \quad (8)$$

where  $f$ —friction factor, which for Reynolds numbers less than 2100 is specified as follows [19]:

$$f = \frac{16}{Re} \quad (9)$$

and for Reynolds numbers exceeding 2100, prescribed as in [19]:

$$f = \frac{0.054}{Re^{0.2}} \quad (10)$$

where Reynolds number is expressed as in [19]:

$$Re = \frac{d_i m}{\mu A_c} \quad (11)$$

Uniting and rearranging (6)–(8) we obtain:

$$L_h = \frac{\Delta P \rho d_i^5 N_t^2 U_p^2 \pi^2}{32f m^2} \quad (12)$$

In order to give the flat plate collector a standard dimension it is necessary to locate in its body an extended heat absorbing tube. If to add to the collector's heat absorbing tube a spiral form, then in the solar collector with a standard body dimension there might be placed the transfer media channel with a length, exceeding a body height several fold. Due to big amount of local resistances the hydraulic losses magnitude will be high. In that connection we forced to use the big capacity circulation pump which will increase financial expenditures. Therefore we shall minimize the hydraulic losses magnitude and at the same time maximize the collector's heat absorbing tubes length. For that purpose there shall be used several heat absorbing tubes, connected between with rack-type tools and other fittings, as it is shown on the **Figure 1**. Such technical solution will broke down the overall flow of the transfer media in the collector into several smaller ones, which, in turn, will reduce amount of the pipeline local resistances, simultaneously having increased the time of the transfer media being under the solar radiation. Apart from that, the given solution will allow increase the transfer media speed, and accordingly, raise its flow, using a circulation pump with less capacity, cutting thereby the financial expenses. Speed increase and transfer media flow will give a possibility to upgrade the heat output factor from a tube to liquid, which, in turn, will increase the solar collector performance.

When water is heated and its density in the collector's circuit is decreased there appears surplus hydrostatic pressure  $P(\Pi a)$

$$\Delta P = g * [\rho_w(t_c(n_c) - \rho_w(t_b))] * F \quad (13)$$

$$F = \frac{d_b + d_c * \sin(S)}{2} + d_{c-b} \quad (14)$$

where  $g$ —gravity acceleration,  $m/s^2$ ;  $F$ —vertical distance between the solar collector and tank-accumulator centers, m;  $d_b$ —tank-accumulator height, m;  $d_c$ —collector's length, m;  $d_{c-b}$ —distance between the tank-accumulator bottom and collector's upper part, m.

Such pressure is balanced with the head loss, caused with total collector circuit hydraulic resistance, consisting of the collector's copper tubular spiral resistances of input and output transfer media of pipelines and devices for their connecting with a collector and tank-accumulator. Upon calculating the pressure losses in the body the hydraulic circuit is broken down into linear and nonlinear parts.

Each element of a copper spiral consists of a linear part and two nonlinear parts (apart from the upper and lower coils, which contain one nonlinear element each).

Overall spiral elements quantity is computed according to a formula:

$$ne = \frac{L - (d_c - 2 * dkk)}{dk - 2 * dkk} \quad (15)$$

where  $dkk$ —distance from the collector's edges to the linear part of the upper and lower spiral elements, m;  $dk$ —distance from the right and left collector's sides to the copper spiral elements, m.

Due to the fact, that the spiral elements amount, in compliance with the collector's constructive properties shall be an integer and even number, the value  $ne$  is rounded off to the nearest even number.

Distance between the spiral elements is defined from the expression:

$$de = \frac{dk - 2 * dkk}{ne} \quad (16)$$

Arc lengths of linear ( $ll$ , m) and nonlinear ( $ln$ , m) parts of the copper spiral element.

$$ln = \pi * \frac{se}{2} \quad (17)$$

$$ll = \frac{L}{de - 2 * ln} \quad (18)$$

Pressure drop in the spiral element linear part is described with an equation:

$$\Delta P = \frac{32\mu(t) * ll}{d^2} * v_{aver} \quad (19)$$

where  $\mu$ —transfer media dynamic viscosity average along the spiral linear part length, H·c/M<sup>2</sup>;  $v_{aver}$ —heat transfer average speed.

Pressure loss in the nonlinear spiral element of the collector is computed from the expression:

$$\Delta P_{ln} = \xi * \frac{v_{aver}}{\rho} \quad (20)$$

where  $\xi$ —local resistance factor.

Collector's nonlinear spiral part local resistance represents the pipe rotation for 90° and it is computed according to the formula

$$\xi = 0.051 + 0.19 \frac{d}{R} \quad (21)$$

where  $R$ —radius of the spiral copper tube rotation m,  $R = se/2$ .



For simulating hydraulic resistances fall in the copper tubular spiral at collector modules, obtained based on the equations.

- at the first area of the collector:

$$H_R = n * \frac{64 * (\mu(t_b(3)) + \mu(t_c(1))) * ll}{\pi * d^4} + (2 * n - 1) * 2\xi * \frac{\rho(t_b(3)) + \rho(t_c(1))}{\pi * d^4} \quad (22)$$

- at  $i$ -m collector's art ( $i = 2, \dots, n_k - 1$ ):

$$H_c(t) = n * \frac{64 * (\mu(t_c(t-1)) + \mu(t_c(t))) * ll}{\pi * d^4} + 4n * \xi * \frac{\rho(t_c(t-1)) + \rho(t_c(i0))}{\pi * d^4} \quad (23)$$

Heat amount  $q_k(\text{Дж})$ , incoming from a collector to a tank-accumulator we will define, using a formula

$$q_c = c_w(t_c) * \rho_w(t_c) * t_c * g_c \quad (24)$$

In flat plate solar collectors heat absorption area and working liquid conditions are not favorable enough, particularly, when the heat receiver (boiler) is placed horizontally. Actually, the liquid motion speed is low here and it is heated from top, and, as a result, convective currents mixing the liquid do not develop. At the boiler's sloping position under known conditions there might happen the natural convection improving the heat transfer [22].

Task solution of heat transfer between radiant heat absorbing surface and power liquid flat heaters upon applying the forced and natural convection (first type boundary conditions) presents sufficient difficulties. In case of applying the natural convection to the forced flow the velocity gradient on the wall will depend on the interrelated parameter part, defining both forced and free flow. In that case velocity gradient  $A = \left(\frac{dW_A}{dy}\right)_{r_0}$  is not known in advance (for circular tube)  $A = \rho \bar{W}/d$ , for flat one  $A = 6\bar{W}/h$ , ( $A$ ) can be defined from the motion equation.

Let us use the motion equation in a simplified form, omitting inertial terms, but taking into account the upward force. Supposing the liquid physical properties being constant and presenting the density in the form of linear temperature, we will obtain [22]:

$$\frac{\partial^2 W_x}{\partial y^2} + \frac{g\beta(t_c - t_0)}{\nu} + \frac{1}{\mu} \frac{\partial P}{\partial x} = 0 \quad (25)$$

where  $\beta$ —volume coefficient;  $t_0$ —flow temperature far from the wall, admitted as equal to the inlet temperature, as within the thermal initial section the temperature in the flow core changes ineffectually.

The equation for temperature distribution is given by [11]:

$$\frac{t - t_c}{t_c - t_0} = \frac{\int_0^n e^{-\eta^3} d\eta}{\int_0^\infty e^{-\eta^3} d\eta} \quad (26)$$

where  $t_c$ —wall temperature,  $\eta = \left(\frac{A}{gdx}\right)_y^{1/3}$   $y$ —new independent variable.

Denominator (26) represents the gamma function, the values of which are tabulated [13]:

$$\int_0^{\infty} e^{-\eta^3} d\eta = \Gamma\left(\frac{3}{4}\right) = 0,8930 \quad (27)$$

Having substituted in (25) the value from (26) and upon integrating it we can define  $A = \left(\frac{dW_x}{dy}\right)_{y=0}$ . To carry out integration we approximate (26) and reduce the equation as follows:

$$\frac{t - t_c}{t_c - t_0} = 1 + b_1 e^{-\eta} + b_2 e^{-2\eta} + b_3 e^{-3\eta} \quad (28)$$

which meets boundary conditions and upon the constants appropriate selection conforms quite well with (25). Having inserted  $t_c - t_0$  from (28) into (25), we find

$$\frac{\partial^2 W_x}{\partial y^2} \cdot \frac{g\beta(t_c - t_0)}{v} (1 + b_1 e^{-\eta} + b_2 e^{-2\eta} + b_3 e^{-3\eta}) - D \quad (29)$$

$$\text{(where) } D = \frac{1}{\mu} \frac{\partial P}{\partial x} \approx \text{const}$$

Boundary conditions are in the following form:  $x = 0, t = t_0$

$$W_x = 6W\left(\frac{Y}{h} - \frac{Y^2}{h^2}\right), W_x = 8W\left(\frac{Y}{d} - \frac{Y^2}{d^2}\right) \quad (30)$$

The first equation is for flat, the second—for circular tube. Having executed integration and used boundary conditions we obtain the expression for nondimensional velocity speed on the wall. For a flat tube

$$\varphi = \frac{Ah^2}{v} = 6Re + 0.43Gr\left(\frac{gx}{Pr\varphi h}\right)^{1/3} \quad (31)$$

$$Re = \frac{\bar{W}h}{v}; Gr = \frac{g\beta(t_c - t_0)h^3}{v^2}$$

Unfortunately, the expression thereof contains non evident  $\varphi$ . Therefore in (31) it was substituted with an approximate relationship:

$$\varphi = 6Re + 0.92 \frac{Gr^{3/4}}{Pr^{1/4}} \left(\frac{\alpha}{h}\right)^{1/4} \quad (32)$$

As you can see, the initial supposition about  $\varphi$  (or  $\bar{A}$ ) consistency is not justified. However,  $\varphi$  changes in length relatively ineffectually ( $\varphi \sim x^{1/4}$ ). Therefore, it will not be a great mistake if to use an average value in the section with the length:

$$\bar{\varphi} = \frac{\bar{A}h^2}{v} 6Re + 0.736 \frac{Gr^{3/4}}{Pr^{1/4}} \left(\frac{e}{h}\right)^{1/4} \quad (33)$$

Let us define now local heat-transfer coefficient, assigning it to the difference between the wall temperature and liquid temperature at the inlet to the heating area. Such definition technique ( $\alpha$ ) is convenient hereby, as at small values  $\frac{1}{Pe} \frac{x}{d}$  the liquid average mass temperature changes weakly in length

$$\alpha_0 = \frac{g_c}{t_c - t_0} = -\frac{\lambda}{t_c - t_0} \left( \frac{dt}{dy} \right)_{y=0} \quad (34)$$

Having used the correlation obtained previously, we find:

$$\left( \frac{dt}{dy} \right)_{y=0} = \left( \frac{A}{gax} \right)^{1/3} \left( \frac{dt}{d\eta} \right)_{\eta=0} = \left( \frac{A}{gax} \right)^{1/3} \left( \frac{t_c - t_0}{0.893} \right) \quad (35)$$

consequently  $\alpha_0$  from (32) and (33)

$$\alpha_0 = \frac{\lambda}{0.893} \left( \frac{A}{9ax} \right)^{1/3} \quad (36)$$

Having substituted the value  $A$  from (10) in (11) we find the expression of Nusselt criterion for flow in a flat tube [18]:

$$Nu = 1.467 \sqrt[3]{Pe \frac{h}{l} + 0.123 \left( GrPr \frac{h}{l} \right)^{3/4}} \quad (37)$$

where  $Nu = \frac{ad}{\lambda}$ ;  $Pe = \frac{\overline{W}d}{\alpha}$ ;  $Gr = \frac{g\beta(t_c - t_0)d^3}{\nu^2}$

In case of flow in a circular tube the similar analysis brings to an expression [18]:

$$Nu = 1,615 \sqrt{Pe \frac{h}{l} + 0,092 \left( GrPr \frac{h}{l} \right)^{3/4}} \quad (38)$$

where  $NU = \frac{ad}{\lambda}$ ;  $Pe = \frac{\overline{W}d}{\alpha}$ ;  $Gr = \frac{g\beta(t_c - t_0)d^3}{\nu^2}$

### 3. Results

For searching the optimal hydraulic regime in the pipeline system of the solar collector, presented on the **Figure 1**, it is necessary to carry out the hydraulic analysis. Its main point is in specifying the total pressure drop in collector tubes and defining optimal offset quantity and, accordingly, the length of heat absorbing tubes in the solar collector body with a square of 2 m<sup>2</sup>. Pressure loss in the pipeline area ( $\Pi_a$ )—linear and local resistances, are found according to the formula (24):

$$\Delta P = RL + z \quad (39)$$

where  $R$ —specific linear pressure losses per 1 m pipeline, Pa/m (depends on the pipeline diameter and water flow passing along those tubes).  $L$ —length of the area being computed, m;  $z$ —local pressure losses in the area, Pa. Defined according to the formula (25):

$$z = \sum \xi \frac{v^2}{2g} \quad (40)$$

where  $g$ —free fall acceleration, m/s<sup>2</sup>;  $v$ —transfer media speed, m/s,  $\sum \xi$ —local resistances factors sum.

Having assumed, that pressure losses in the areas A–G and A'–G' is a constant magnitude, the hydraulic computation has been executed only for one standard coil and reduced to a **Table 2**. As a designed consumption value there has been selected the minimal magnitude of the circulation pump consumption with a minimal capacity UPS 25-40 (**Table 3**).

**Figure 2.** Hydraulic computation of heat absorbing tubes of a solar collector with several tubes.

As it is seen from the **Figures 1** and **5**, the values of total pressure losses will not allow using a low capacity pump, which will bring to increasing the heating system cost. Using bigger diameter tubes will allow cutting the total pressure losses, but it will considerably increase the solar collector cost. If to draw attention to the formulae (13) and (14), then we can see, that along with increasing the collector's insulated edge width, performance of the solar collector rectangular profile direct edge is reduced, and therefore reduced also the solar collector efficiency. Then it may be concluded, that using several collector tubes with less edge size allows upgrade the flat solar collector efficiency (**Figure 6**).

When using one pipe with the edge of a flat solar collector, the efficiency of the entire collector area will appear. That is, from **Figures 7** and **8** it can be seen that the water flow in the heat-absorbing single tube of a flat solar collector depends on the sum of the local resistance coefficients, which is an exponential function that increases to a critical maximum of the water velocity (**Figures 9–12**).

Using one tube as an edge of a flat plate solar collector is the efficiency of an overall collector square. That is, from the **Figures 7** and **8** it is seen, that the water consumption in one heat absorbing tube of a flat plate collector from the sum of the local resistance factors is an exponential function, which grows to the critical maximum water speed.

**Figure 13** demonstrates the pressure loss in the linear part of the flat plate solar collector spiral element. It is known, that the pressure fall is an important factor for the thermosyphon systems performance. Accordingly, in the work herein a flat plate solar collector is being studied for predicting the pressure fall on it. Various dimensions collectors have been used as a control example, in which the model has been tested within 3–8% in terms of normalized mean square deviation.

**Figure 14** demonstrates total amount of spiral elements of the flat solar collector copper spiral element. From the figure it is clear, that the more quantity of a flat plate solar collector copper spiral elements, the bigger the distance from the collector edges to the linear upper and lower spiral elements.

The study of convective heat transfer in flat solar collectors is considered, as can be seen from the analysis of heat transfer studies using round and flat pipes with matching forced and free convection, vertically or horizontally, with different liquids; flow direction (**Figure 15**).

Upon specifying the coefficient of heat transfer from the heating area to the heated water the thermal flow is defined according to the flow rate and temperature difference of the water being heated at outlet and inlet. Water temperature is specified at outlet and inlet and the surface temperature through thermocouples readings average [22].

Experiments have been carried out at the heat transfer surface's obliquing angles  $\phi = 30^\circ, 35^\circ, 40^\circ$ .

At that, the number  $Re = 150\text{--}500$ , i.e., the experiments have been executed mainly at water flow laminar regime.

As a determining temperature there has been accepted the water temperature and as a characteristic dimension—the channel equivalent diameter  $d = 4f/S$ .

Accepted in the model dimension  $d$  secures its geometric similarity to experimental flat solar collectors.

Area	Water flow G, л/с	Area length L, m	Outer diameter D, mm	Water speed V, m/s	Specific linear pressure losses, Pa	Linear pressure losses RL, Pa	Local resistances factors sum $\sum \zeta$	Pressure losses on local resistances Z, Pa	Total pressure losses $\Delta P, Pa$	Local resistances factors sum $\xi$
A-A'	0.08	6	7	0.08	345	1850	20	3020	4501.2	0.68

**Table 2.**  
Hydraulic computation of heat absorbing tubes of a solar collector with several tubes.

Area	Water flow G, л/с	Area length L, m	Outer diameter D, mm	Water speed V, m/s	Specific linear pressure losses, Pa	Linear pressure losses RL, Pa	Factors sum in local resistances $\sum \zeta$	Pressure losses on local resistances Z, Pa	Total pressure losses $\Delta P, Pa$	Local resistances factors sum $\xi$
A-A'	0.34	30	10	2.5	Tube diameter 10 mm	87,000	20.45	40215.00	125,460.00	0.68
A-A'	0.34	28	20	1.5	Tube diameter 20 mm	10,421	16.45	7545.00	20,156.00	0.68

**Table 3.**  
Hydraulic computation of heat absorbing tubes of a solar collector with one tube.



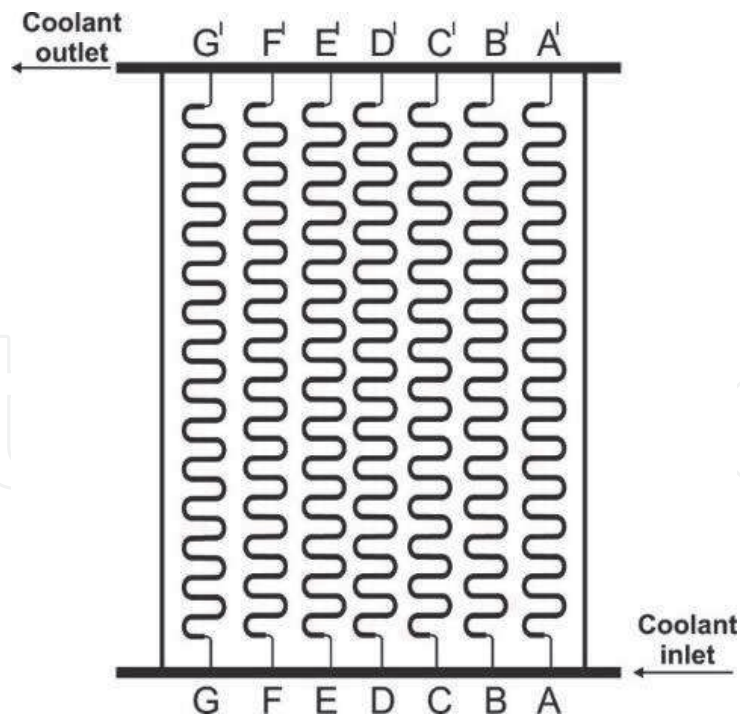


**Figure 5.**  
 Diagrammatic representation of flat plate solar collector with extended heat absorbing tubes.

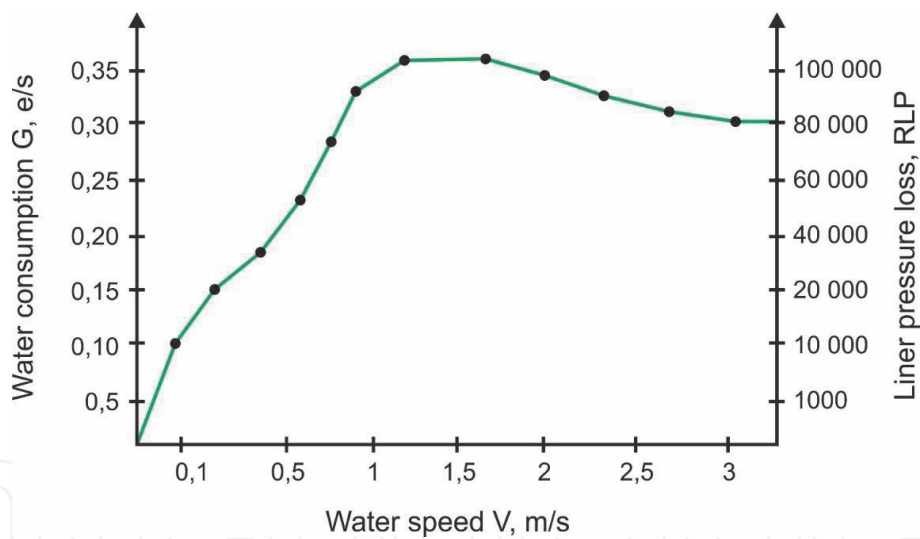


**Figure 6.**  
 Dependence of water consumption on the water flow and linear pressure drops of heat absorbing tubes of the flat solar collector with several tubes [12].

In the result, experimental data in the dependency form  $Nu = f(Pld/l)$  and  $Nu/Pr^{0.44} = f(Re)$  is given in the **Figures 16** and **17** [22].

**Figures 16** and **17** show number for the liquid plays an important role in the points spacing as regard to the curve. In all cases, the lines are with a slope 1/3, as in the research herein we have considered only laminar mode [22].

Obtained semiempirical formula allowing, in concept, processing and summarizing accumulated experimental data on the heat transfer upon convective heat transfer in the flat plate solar collectors as well gives a possibility to compare the results of theoretical investigations of heat transfer characteristics to experimental data.

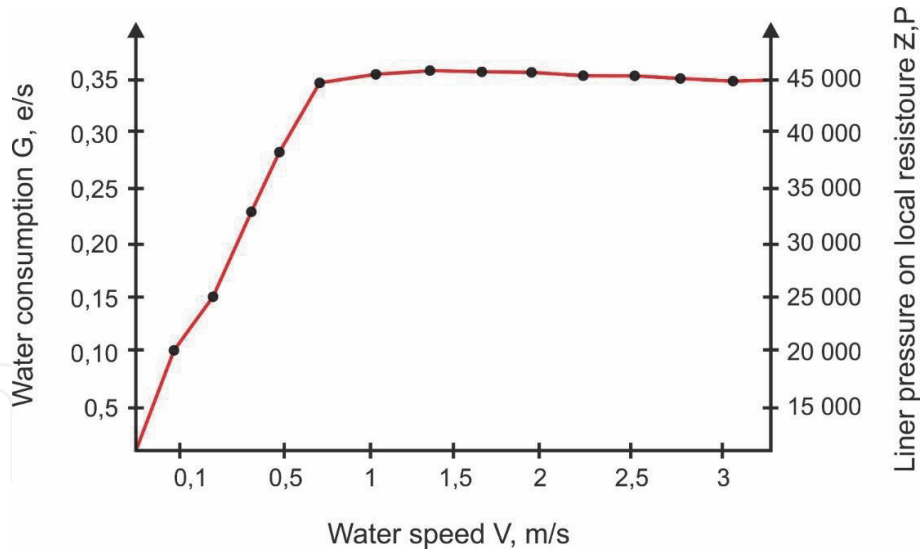


**Figure 7.**  
Dependence of water consumption on the speed and losses on local resistances of heat absorbing tubes of flat solar collector with several tubes.

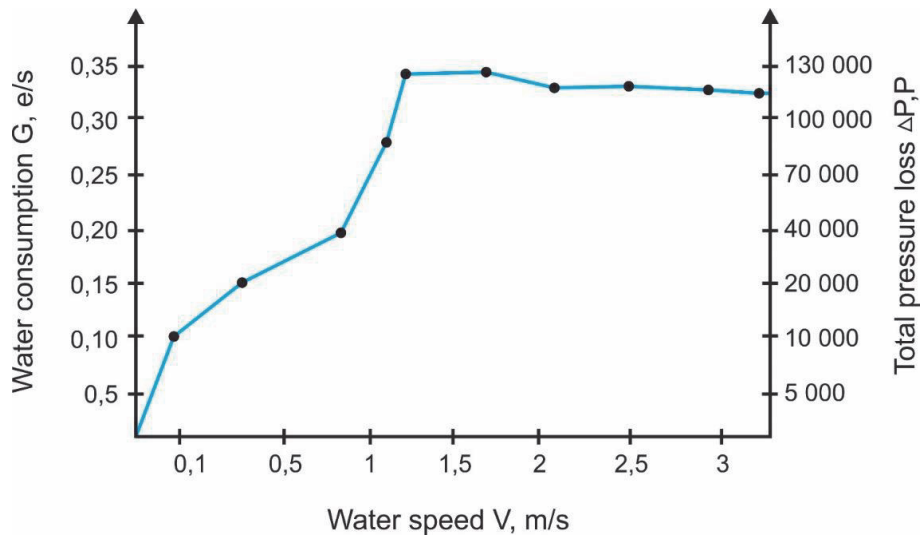


**Figure 8.**  
Dependence of water consumption on the speed and total pressure losses of heat absorbing tubes of flat solar collector with several tubes.

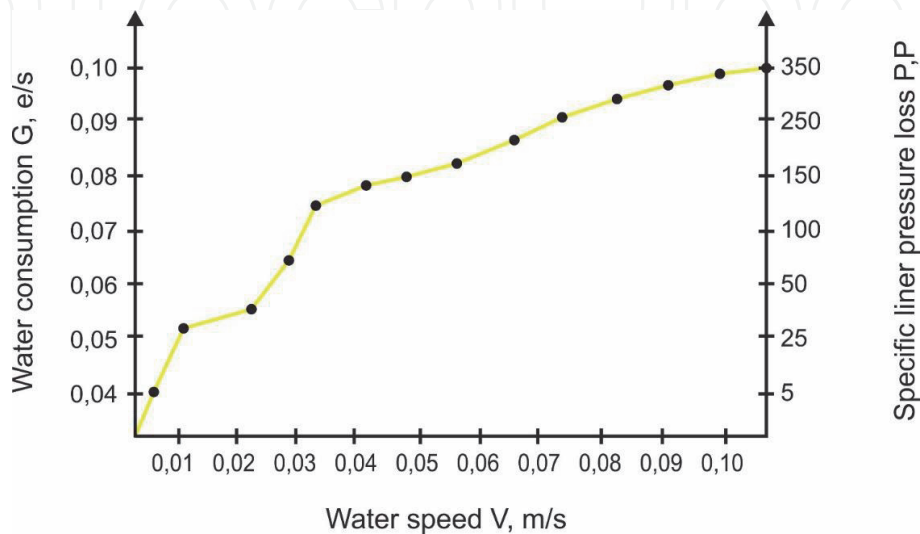


**Figure 9.**  
Dependence of water consumption on the speed and specific linear pressure losses of heat absorbing tubes of flat solar collector with several tubes [21].

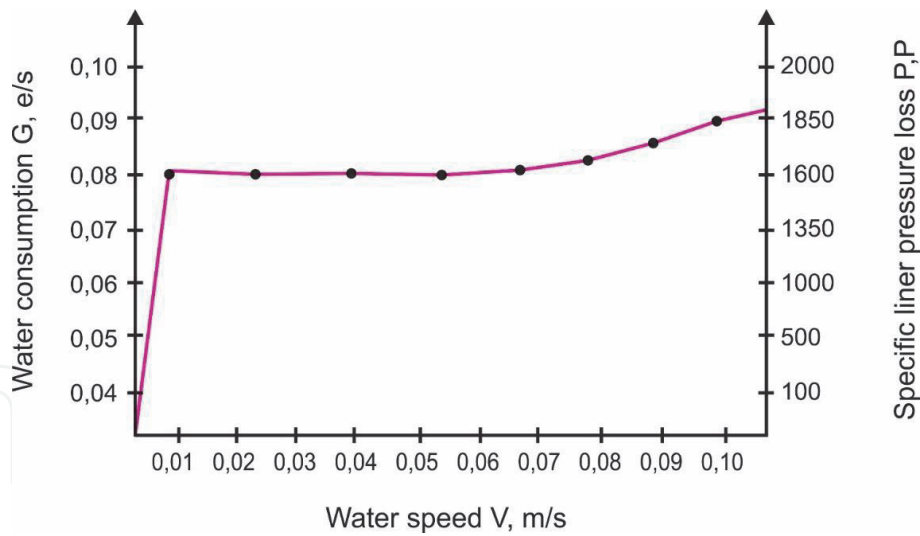


**Figure 10.**  
 Dependence of water consumption on the speed and specific linear pressure losses of heat absorbing tubes of flat solar collector with one tube.

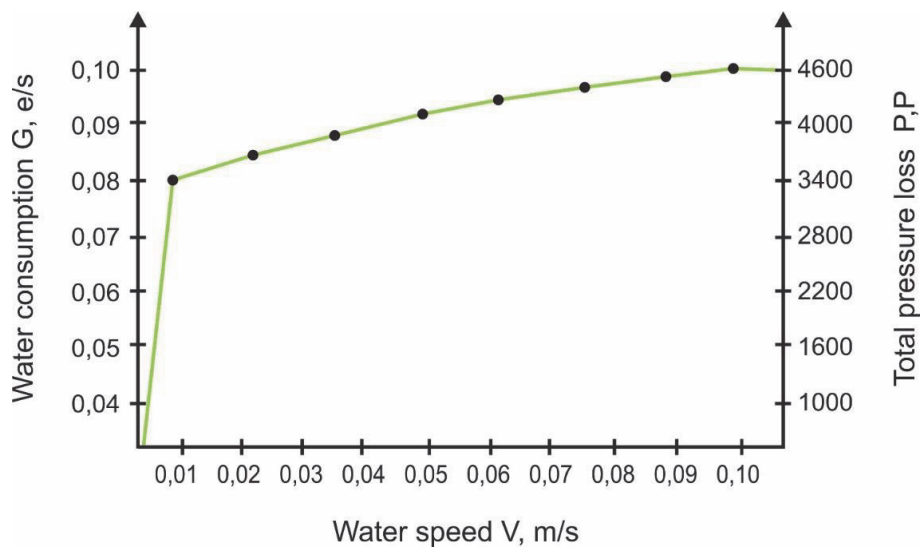


**Figure 11.**  
 Dependence of water consumption on the speed and total pressure losses of heat absorbing tubes of flat solar collector with one tube.

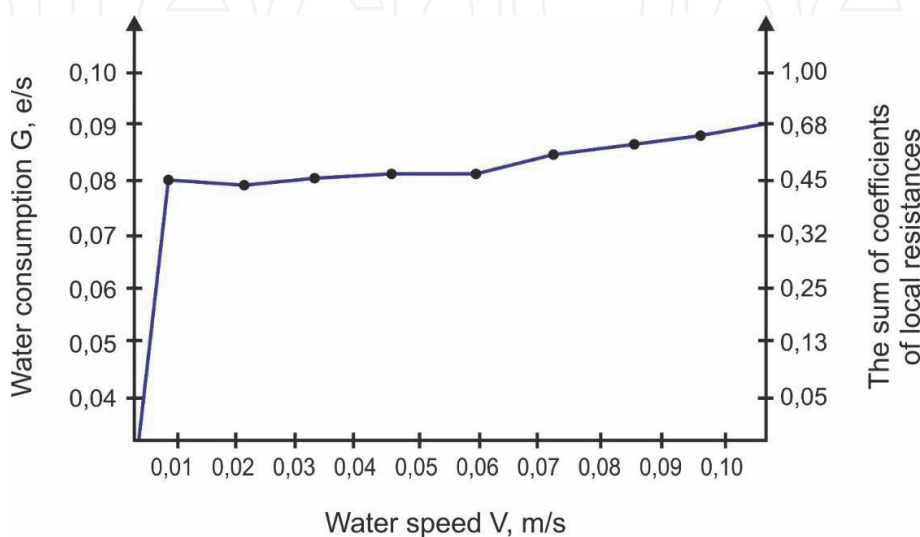


**Figure 12.**  
 Dependence of water consumption on the speed and local resistances factors of heat absorbing tubes of flat solar collector with one tube [21].

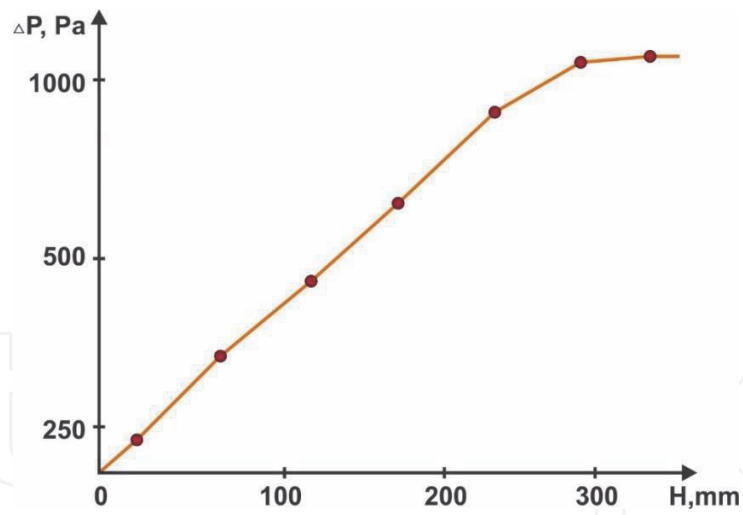


**Figure 13.**  
Pressure loss in linear part of flat plate solar collector's spiral element linear part.

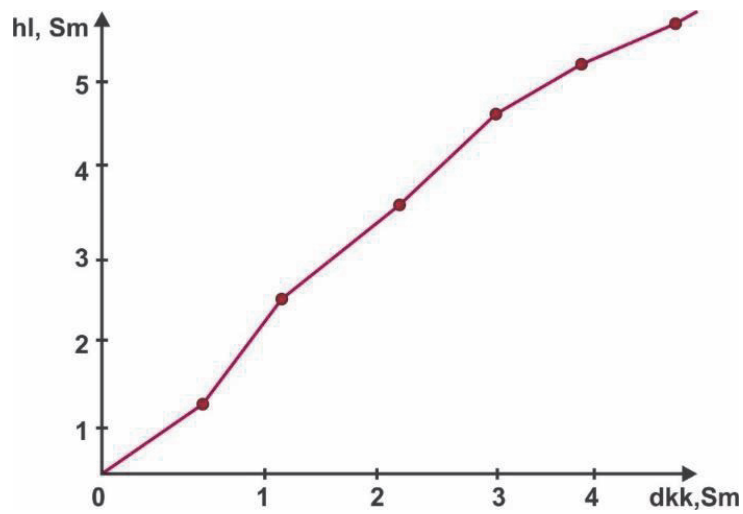


**Figure 14.**  
Total amount of flat plate solar collector's copper spiral elements.

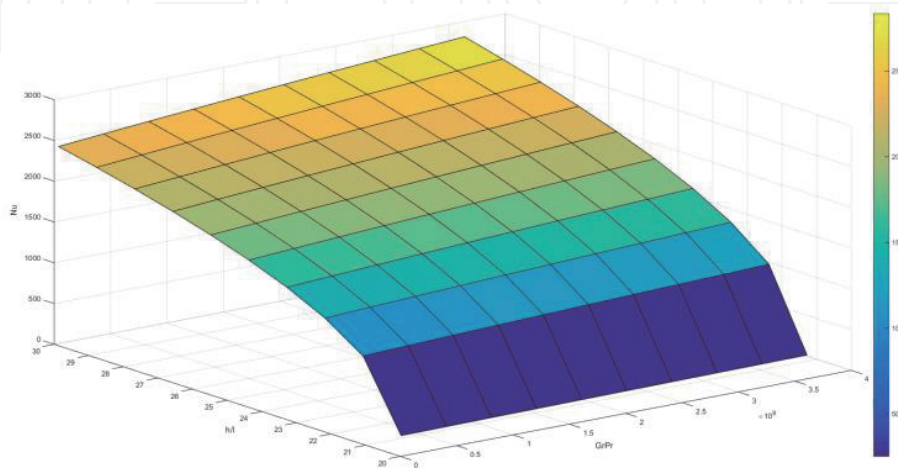


**Figure 15.**  
Nusselt criterion for liquid flow in flat tube [21].



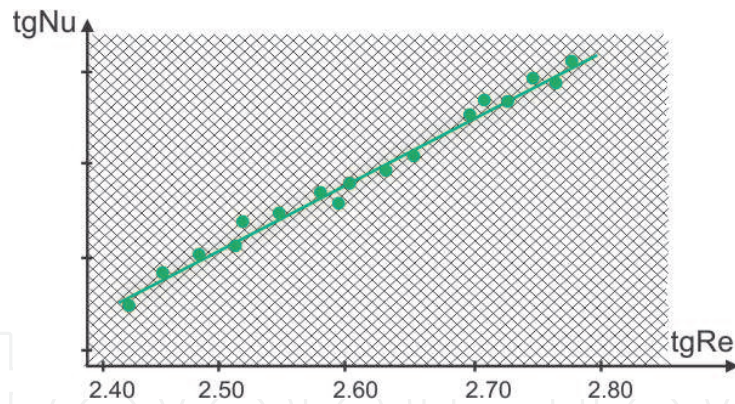


**Figure 16.** Nusselt criterion dependence on Reynolds criterion for liquid flow in the flat solar collector [22].

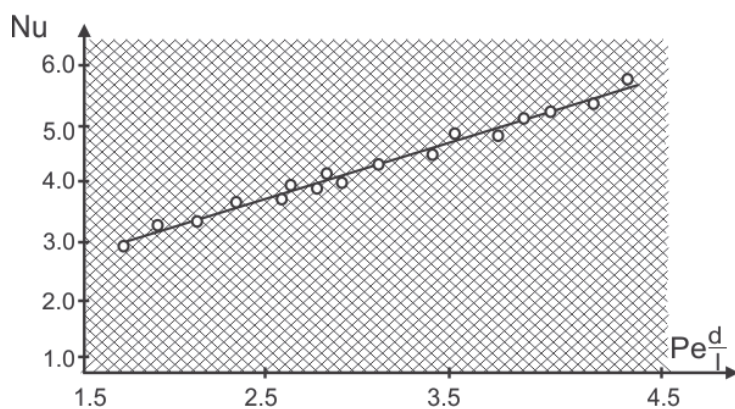


**Figure 17.** Dependence of Nusselt-Prandtl criterion on Reynolds criterion for the liquid flow in the flat plate solar collector [22].

## 4. Conclusion

Flat plate solar collector heat absorbing tubes hydraulic analysis has shown, that using the standard size transfer media channels we can place a pipeline, the length of which 2.5-fold bigger than the collector's body length, and at that, the time of the transfer media being under solar radiation considerably increases. At that, the overall pressure losses in the collector's pipeline turned out to be relatively low, which allows increasing the transfer media speed with the aim to transfer from laminar flow to turbulent, which in its turn, raises the heat output factor from a tube to the liquid, and consequently, also, the flat plate solar collector's efficiency. Apart from that, the calculations have proved, that the optimal hydraulic regime, necessary for securing all above mentioned conditions in the pipeline system having been elaborated, can create even the least powerful circulating pump. As well, in the process of research it has been stated, that making use of several tubes will upgrade the performance of a flat plate solar collector.

Obtained semi empiric formulae, which allow, in principle, processing and generalizing accumulated experimental data on heat transfer at convective heat transfer in flat plate solar collectors, as well they give a possibility to compare the theoretical researches outcomes of various heat transfer characteristics to experimental data [22].



IntechOpen

### Author details

Yedilkhan Amirgaliyev<sup>1,2</sup>, Murat Kunelbayev<sup>1,2\*</sup>, Kalizhanova Aliya<sup>1,2</sup>,  
Ainur Kozbakova<sup>1,2</sup>, Omirlan Auelbekov<sup>1</sup> and Nazbek Katayev<sup>1</sup>


1 Institute of Information and Computing Technologies CS MES RK, Kazakhstan

2 Al-Farabi Kazakh National University, Kazakhstan

\*Address all correspondence to: [murat7508@yandex.kz](mailto:murat7508@yandex.kz)

### IntechOpen

---

© 2020 The Author(s). Licensee IntechOpen. Distributed under the terms of the Creative Commons Attribution - NonCommercial 4.0 License (<https://creativecommons.org/licenses/by-nc/4.0/>), which permits use, distribution and reproduction for non-commercial purposes, provided the original is properly cited. 

## References

- [1] Carravetta A, Del Giudice G, Fecarotta O, Ramos HM. PAT design strategy for energy recovery in water distribution networks by electrical regulation. *Energies*. 2013;**6**:411-424
- [2] Eisenmann W, Vajen K, Ackermann H. On the correlations between collector efficiency factor and material content of parallel flow flat-plate solar collectors. *Solar Energy*. 2004;**76**(4):381-387
- [3] Garg HP. Design and performance of a large scale size solar water heater. *Solar Energy*. 1973;**14**:303-312
- [4] Karagiorgas M, Botzios A, Tsoutsos T. Industrial solar thermal applications in Greece Economic evaluation, quality requirements and case studies. *Renewable and Sustainable Energy Reviews*. 2001;**5**:157-173
- [5] Kiraly A, Pahor B, Kravanja Z. Integration of renewables for improving companies' energy supplies within regional supply networks. *Chemical Engineering Transactions*. 2012;**29**:469-474
- [6] Lin WM, Chang KC, Yi-Mei Liu YM, Chung KM. Field surveys of non-residential solar water heating systems in Taiwan. *Energies*. 2012;**5**:258-269
- [7] Liu YM, Chung KM, Chang KC, Lee TS. Performance of thermosyphon solar water heaters in series. *Energies*. 2012;**5**:3266-3278
- [8] Quijera JA, Garcia A, Labid J. Integration of solar thermal energy and heat pump in a fish canning process combining pinch and exergy analysis. *Chemical Engineering Transactions*. 2012;**29**:1207-1212
- [9] Zago M, Casalegno A, Marchesi R, Rinaldi F. Efficiency analysis of independent and centralized heating, systems for residential buildings in Northern Italy. *Energies*. 2011;**4**:2115-2131
- [10] Amirgaliyev Y, Kunelbayev M, Kalizhanova A, Auelbekov O, Katayev N, Kozbakova A. Theoretical and mathematical analysis of double circuit solar station with thermo siphon circulation. *Journal of Polytechnic-Politeknik Dergisi*. 2019;**22**(2):485-493
- [11] Priyam A, Chand P. Thermal and thermohydraulic performance of wavy finned absorber solar air heater. *Solar Energy*. 2016;**130**:250-259
- [12] Hegazy AA. Thermohydraulic performance of air heating solar collectors with variable width, flat absorber plates. *Energy Conversion and Management*. 2000;**41**:1361-1378
- [13] Ahmad A, Saini JS, Varma HK. Thermohydraulic performance of packed bed solar air heaters. *Energy Conversion*. 1996;**37**:205-214
- [14] Prasad BN, Kumar A, Singh KDP. Optimization of thermo hydraulic performance in three sides artificially roughened solar air heaters. *Solar Energy*. 2015;**111**:313-319
- [15] Balaji S, Saravanakumar K, Sakthivel M, Siva Kumar P. Thermo hydraulic performance of a forced convection solar air heater using pin-fin absorber surface. *International Journal of Advanced Technology in Engineering and Science*. 25 November 2015;**3**(11):360-368
- [16] Verma SK, Prasad BN. Investigation for the optimal thermo hydraulic performance of artificially roughened solar air heaters. *Renewable Energy*. 2000;**20**:19-36
- [17] Mittall MK, Varshney L. Optimal thermo hydraulic performance of a wire

mesh packed solar air heater. *Solar Energy*. 2005;**80**:1112-1120

[18] Behura AK, Rout SK, Pandya H, Kumar A. Thermal analysis of three sides artificially roughened solar air heaters. *Energy Procedia*. 2017;**109**: 279-285

[19] Sourbron M, Ozalp N. Determination of heat transfer characteristics of solar thermal collectors as heat source for a residential heat pump. *Journal of Solar Energy Engineering*. 2016;**138**:1-8

[20] Ziemelis I, Kancevica L, Jesko Z, Putans H. Calculation of energy produced by solar collectors. *Engineering for Rural Development*. 2009:212-2018

[21] Chabane F, Moumami N, Benramache S. Experimental study of heat transfer and thermal performance with longitudinal fins of solar air heater. *Journal of Advanced Research*. 2014; **5**(2):183-192

[22] Amirgaliyev Y, Kunelbayev M, Kalizhanova A, Auelbekov O, Kataev N. Study of convective heat transfer in flat plate solar collectors. *WSEAS Transactions on Systems and Control*. 2019;**14**:129-137